Contract No:

This document was prepared in conjunction with work accomplished under Contract No. DE-AC09-08SR22470 with the U.S. Department of Energy (DOE) Office of Environmental Management (EM).

Disclaimer:

OPC PASTE SAMPLES EXPOSED TO AGGRESSIVE SOLUTIONS

Cementitious Barriers Partnership

November 2014

CBP-TR-2015-001, Rev. 0

CEMENTITIOUS BARRIERS PARTNERSHIP
TASK 12 – EXPERIMENTAL STUDY

OPC Paste Samples Exposed to Aggressive Solutions

Yannick Protière, M.Sc., jr. eng.
Eric Samson, Ph.D., eng.

SIMCO Technologies, Inc.
Québec, Canada

November 2014

CBP-TR-2015-001, Rev. 0

ACKNOWLEDGEMENTS

This report was prepared for the United States Department of Energy in part under Contract No. DE-AC09-08SR22470 and is an account of work performed in part under that contract. Reference herein to any specific commercial product, process, or service by trademark, name, manufacturer, or otherwise does not necessarily constitute or imply endorsement, recommendation, or favoring of same by Savannah River Nuclear Solutions or by the United States Government or any agency thereof. The views and opinions of the authors expressed herein do not necessarily state or reflect those of the United States Government or any agency thereof. The authors would like to acknowledge the contributions of Elmer Wilhite of Savannah River National Laboratory, David Kosson of Vanderbilt University and CRESP, Jake Philip of the U.S. Nuclear Regulatory Commission, and Ed Garboczi of the National Institute of Standards and Technology for contributions to the document. They would also like to acknowledge the contributions of Media Services of Savannah River Nuclear Solutions and Savannah River National Laboratory personnel for editing and assistance with production of the document.

and

This report is based on work supported by the U. S. Department of Energy, under Cooperative Agreement Number DE-FC01-06EW07053 entitled 'The Consortium for Risk Evaluation with Stakeholder Participation III' awarded to Vanderbilt University. The opinions, findings, conclusions, or recommendations expressed herein are those of the author(s) and do not necessarily represent the views of the U.S. Department of Energy or Vanderbilt University.

DISCLAIMER

Printed in the United States of America

United States Department of Energy
Office of Environmental Management
Washington, DC

This document is available on the U.S. DOE Information Bridge and on the CBP website: http://cementbarriers.org/
An electronic copy of this document is also available through links on the following websites: http://srnl.doe.gov/ and http://cementbarriers.org/

FOREWORD

The Cementitious Barriers Partnership (CBP) Project is a multi-disciplinary, multi-institutional collaboration supported by the United States Department of Energy (US DOE) Office of Waste Processing. The objective of the CBP project is to develop a set of tools to improve understanding and prediction of the long-term structural, hydraulic, and chemical performance of cementitious barriers used in nuclear applications.

A multi-disciplinary partnership of federal, academic, private sector, and international expertise has been formed to accomplish the project objective. In addition to the US DOE, the CBP partners are the Savannah River National Laboratory (SRNL), Vanderbilt University (VU) / Consortium for Risk Evaluation with Stakeholder Participation (CRESP), Energy Research Center of the Netherlands (ECN), and SIMCO Technologies, Inc. The Nuclear Regulatory Commission (NRC) is providing support under a Memorandum of Understanding. The National Institute of Standards and Technology (NIST) is providing research under an Interagency Agreement. Neither the NRC nor NIST are signatories to the CRADA.

The periods of cementitious performance being evaluated are >100 years for operating facilities and > 1000 years for waste management. The set of simulation tools and data developed under this project will be used to evaluate and predict the behavior of cementitious barriers used in near-surface engineered waste disposal systems, e.g., waste forms, containment structures, entombments, and environmental remediation, including decontamination and decommissioning analysis of structural concrete components of nuclear facilities (spent-fuel pools, dry spent-fuel storage units, and recycling facilities such as fuel fabrication, separations processes). Simulation parameters will be obtained from prior literature and will be experimentally measured under this project, as necessary, to demonstrate application of the simulation tools for three prototype applications (waste form in concrete vault, high-level waste tank grouting, and spent-fuel pool). Test methods and data needs to support use of the simulation tools for future applications will be defined.

The CBP project is a five-year effort focused on reducing the uncertainties of current methodologies for assessing cementitious barrier performance and increasing the consistency and transparency of the assessment process. The results of this project will enable improved risk-informed, performance-based decision-making and support several of the strategic initiatives in the DOE Office of Environmental Management Engineering & Technology Roadmap. Those strategic initiatives include 1) enhanced tank closure processes; 2) enhanced stabilization technologies; 3) advanced predictive capabilities; 4) enhanced remediation methods; 5) adapted technologies for site-specific and complex-wide D&D applications; 6) improved SNF storage, stabilization and disposal preparation; 7) enhanced storage, monitoring and stabilization systems; and 8) enhanced long-term performance evaluation and monitoring.

Christine A. Langton, PhD
Savannah River National Laboratory

David S. Kosson, PhD
Vanderbilt University / CRESP

EXECUTIVE SUMMARY

The study presented in this report focused on a low-activity wasteform containing a high pH pore solution with a significant level of sulfate. The purpose of the study was to improve understanding of the complex concrete/wasteform reactive transport problem, in particular the role of pH in sulfate attack.

Paste samples prepared at three different water-to-cement ratios were tested. The mixtures were prepared with ASTM Type I cement, without additional admixtures. The samples were exposed to two different sodium sulfate contact solutions. The first solution was prepared at 0.15M Na_2SO_4. The second solution also incorporated 0.5M NaOH, to mimic the high pH conditions found in Saltstone.

After three months of exposure, various techniques were used to quantify the penetration of sulfate in the paste samples and the damage sustained as a result of sulfate exposure:

- Layer-by-layer analysis of sulfate content through acid dissolution,
- Microprobe analysis,
- Mercury intrusion porosimetry,
- X-ray diffraction.

The data collected indicated that in Na_2SO_4 solution, damage occurs to the pastes. Sulfate profiles, either from layer-by-layer acid dissolution analysis or by microprobe, confirm the penetration of sulfate in the material. Limited XRD data show that in the damaged portion next to the surface, ettringite and gypsum was formed. Alterations to the microstructure were confirmed by MIP measurements. Close to the surface, where the paste is most damaged, some of the finer pores were filled, as indicated by a reduction of the pore volume in the 10nm-100nm pore range. However, for pores in the 20nm–2μm pore range, pore volume increased. This newly created volume can be associated with microcracks, likely created by the formation of ettringite and gypsum. These observations are valid for all three paste mixtures. The rate of sulfate ingress and degradation was directly related to the mix characteristics: higher water-to-cement ratio showed higher rates of degradation.

In the case of the high pH sulfate solution (Na_2SO_4 + NaOH), no signs of damage was observed on any of the paste mixtures. Contrary to the previous case, the deleterious mineral phases associated with sulfate exposure did not form in the high pH environment. A possible explanation for this is the absence of gypsum formation at high pH. Similar conclusions were drawn on the basis of numerical simulations in Task 7 of the CBP project.

Although these results need further confirmation, they indicate that the high sulfate content found in the wasteform pore solution will not necessarily lead to severe damage to concrete. Good quality mixtures could thus prove durable over the long term and act as an effective barrier to prevent radionuclides from reaching the environment. Additional experiments with contact solutions that mimic more closely wasteform pore solution are needed to confirm this.

CONTENTS

LIST OF FIGURES

LIST OF TABLES

1.0 OBJECTIVE

This report summarizes the first series of experimental work performed by SIMCO Technologies Inc. (SIMCO) during the Cementitious Barriers Partnership (CBP) project. The test series is referred to as Phase I for the remainder of the report.

Concrete barriers are viewed as a potential solution to store a contaminated wasteform resulting from nuclear material production processes. In this context, concrete is expected to act as a contaminant barrier for an extended period of time. Wasteform in direct contact with concrete can compromise the integrity of the barrier due to the potentially high concentration of deleterious ionic species it contains.

The study presented in this report focused on low-activity wasteform containing a high pH pore solution with a significant level of sulfate. The purpose of the study was to improve understanding of the complex concrete/wasteform reactive transport problem, in particular the role of pH in sulfate attack.

The study was initially intended as the initial phase of a more complete experimental program. The main objective was to gather data that would help pinpoint the choice of materials and exposure solutions of the next research phase. With this in mind, it was decided to test samples already available at SIMCO from past studies. Paste samples prepared a few years earlier and kept in controlled curing chambers were thus used for the present project. The samples were immersed in sulfate contact solutions and analyzed to measure the impact of the aggressive environment on the material.

This report summarizes the characterization study performed on three hardened ASTM Type I cement pastes mixtures exposed to 1) a neutral-pH and 2) a basic-pH solutions, both containing a high level of sulfate.

The report is divided as follows: Section 2 presents the characteristics of raw materials. Section 3 details the formulations and the method of preparation of the mixtures. Section 4 presents pore structure properties measurements performed on the mixtures. Section 5 presents the results of samples immersed in high-sulfate contact solutions and the associated pore structure alteration observed.

2.0 RAW MATERIALS

This section presents the characteristics of the cement used in the paste mixtures.

All paste samples were prepared with the same ASTM Type I cement. The chemical composition is given in Table 1. It was evaluated using the X-ray fluorescence technique.

Table 1 – Chemical composition of cement (% mass)

Oxides	Type I cement
CaO	63.7
SiO_2	19.4
Al_2O_3	5.21
Fe_2O_3	2.34
SO_3	2.3
MgO	2.29
K_2O	0.84
Na_2O	0.25
L.O.I	3.11

The relative density (specific gravity) of this Type I cement is 3.09.

3.0 HYDRATED PASTE MIXTURES

Three hydrated cement pastes, identified as P1, P2, P3 having respectively water-to-cement ratios of 0.50, 0.65, 0.75, were prepared. Even though mixtures used for waste storage are prepared at a lower w/c ratio, having high-w/c mixes on hand allowed reducing the time of testing due to increased porosity and diffusivity.

Table 2 – Hardened cement paste mixtures

Materials	Quantity (kg)		
	P1	P2	P3
Water-cement ratio	0.50	0.65	0.75
Cement Type I	380	280	250
Water	190	182	188

Materials were prepared in a 2-liter mixer placed in a vacuum chamber in order to limit air bubble formation. Cylindrical specimens of 4 inches in diameter (Ø100×200mm or Ø4" ×8") were cast from each batch in accordance with the ASTM Standard C305 - Mechanical Mixing of Hydraulic Cement Pastes and Mortars of Plastic Consistency. After casting, molds were sealed, placed horizontally in a setup where they were affixed to a rotating wheel. Following this, they were rotated on their axis during the first 24 hours after mixing in order to limit bleeding.

After rotation, the cylinders were demolded and stored in a moist room (100% RH) during 4 years.

4.0 PASTE PROPERTIES MEASUREMENTS

The following pore structure properties of hardened cement pastes were determined:

- Chemical composition of pore solution.

- Porosity: measured in accordance with the ASTM Standard C642 - Standard Test Method for Density, Absorption, and Voids in Hardened Concrete applied to hardened cement pastes.
- Desorption isotherm: estimated by mass loss measurements, based on procedure detailed in appendix A.
- Pore size distribution: evaluated from Mercury Intrusion Porosimetry (MIP) measurements.

The following sections present a brief description of the testing methods and the results obtained for each paste mixture.

4.1. Chemical composition of expressed pore fluids

The pore solution extraction procedure consists in applying sufficient pressure on a concrete sample to extract the solution from the material. Pore solution was extracted by squeezing the crushed samples under compressive loading using the device shown in Figure 1. Solution was delivered through a drain ring and channel and recovered with a syringe in order to limit the exposure to the atmosphere. Pore solution analyses were carried out shortly after the extraction tests.

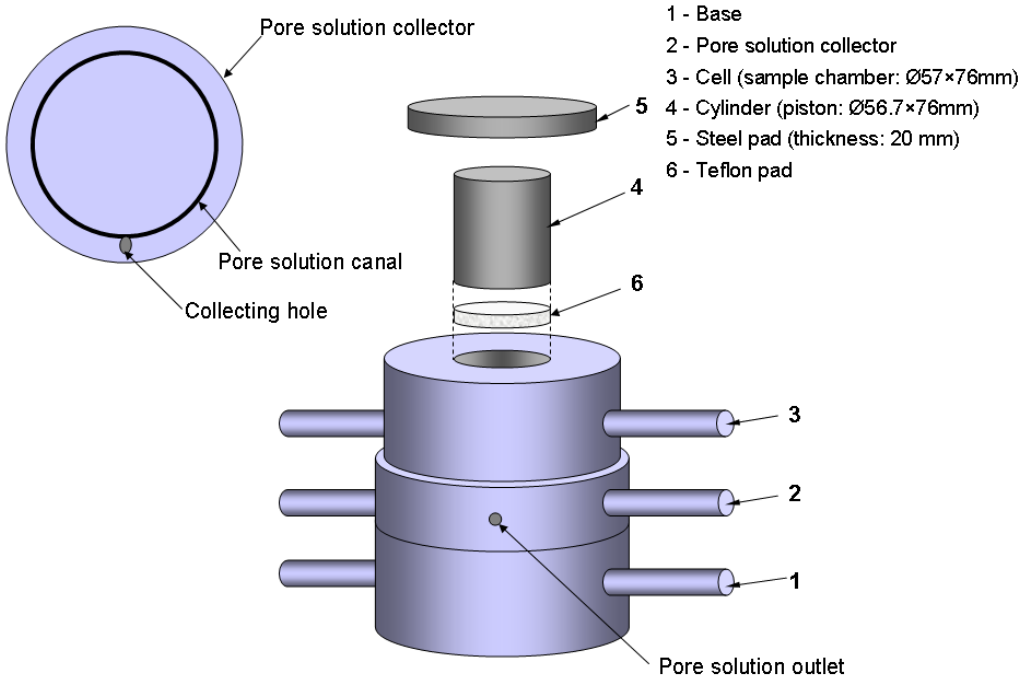

Figure 1 – Experimental setup for pore solution extraction

Pore solution extractions were made on the hardened cement pastes prior to the present test series, after 56 days of curing. The specimens for pore solution extraction were sawn from cylinders. Samples were broken in small pieces, placed in the cell, and crushed at a high pressure. Pore solution analyses were carried out shortly after extraction by Atomic Absorption Analyzer and Ion Chromatography as well as pH titrator to obtain the contents of the main ions in the pore solution: OH^-, Na^+, K^+, SO_4^{2-}, Ca^{2+}, Cl^-. Table 3 presents the results of the chemical composition of expressed pore fluids.

It should be noted that the results listed in Table 3 are not strictly neutral. This is a result of experimental errors associated with the procedure.

Table 3 - Chemical analyses of pore fluids extracted after 56 days of curing, [mmol/L]

Mixture	Age	OH^-	Na^+	K^+	Ca^{2+}	$SO4^{2-}$	Cl^-
P1	56 days	255.4	78.3	158.6	1.8	2.1	1.8
P2	56 days	154.0	47.8	84.4	3.0	0.2	2.9
P3	56 days	131.1	32.2	66.5	2.5	0.4	3.2

4.2. Porosity measurements

The porosity measurements were performed on the basis of the ASTM C642 standard procedure: Standard Test Method for Density, Absorption and Voids in Hardened Concrete. The porosity results and associated mass water contents and densities are given in Table 4**.**

Values presented in Table 4 show that porosities increase with the water-cement ratio. Saturated mass water contents are expressed per mass of dried (g_d) and saturated (g_{sat}) hardened cement paste. Associated pastes densities are also presented.

Table 4 – Hardened cement pastes properties after 56 days of curing

Description	P1	P2	P3
Porosity (volume of permeable voids) [%]	46.9%	54.4%	58.7%
Saturated mass water content, per mass of dried sample [g/g_d]	0.329	0.450	0.533
Saturated mass water content, per mass of saturated sample [g/g_{sat}]	0.247	0.304	0.348
Dry density [g_d/cm^3]	1.43	1.18	1.10
Saturated density [g_{sat}/cm^3]	1.89	1.75	1.69

4.3. Desorption isotherm

Tests for desorption isotherms were performed on thin samples cut from cylinders after 56 days of hydration in the fog room. The samples were then immersed under water during seven days to improve the saturation of the material. The thin samples were placed in different RH-controlled boxes: 11.3%, 33.1%, 54.4%, 75.5%, 85.1%, 91.0%, 94.6%, and 97.3%. At least three samples per relative humidity conditions and per mixture were prepared. Measurements are based on the test procedure detailed in Appendix A. An average desorption isotherm, expressed in gram of water per gram of dried cement paste versus relative humidity is presented in Figure 2 for each mixture. Using the Kelvin relationship presented below, it is possible to substitute the relative humidity by the capillary pressure:

$$p_c = -\frac{\rho_l RT}{M_w}\ln(RH)$$

where M_w is the molar mass of water, ρ_l is the density of liquid water, taken as 1000.0 kg/m^3, R is the ideal gas constant and T is the temperature. Moisture retention functions expressed as relative humidity and capillary pressure are plotted in Figure 2.

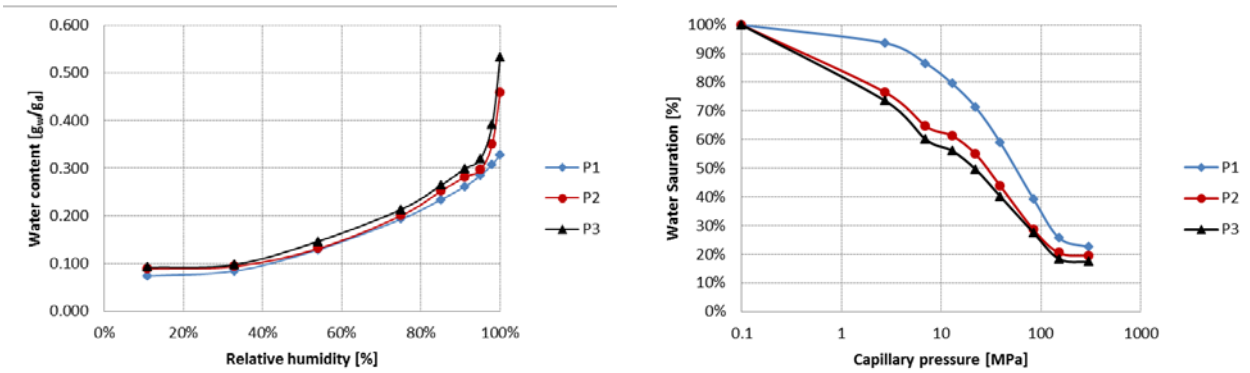

a) Expressed as water content vs. RH b) Expressed as water saturation vs. p_c

Figure 2 – Desorption isotherm of hardened cement pastes at 23°C

Desorption results presented in Figure 2 clearly show the effect of water-cement ratio on the water content value. Increasing water-to-cement ratios increases the capillary pore volume, implying larger saturated water content values.

4.4. Mercury Intrusion Porosimetry (MIP)

The determination of the pore size distribution is commonly performed by Mercury Intrusion Porosimetry (MIP).

The MIP experiment is based on the physical principle that a non-reactive, non-wetting liquid, such as mercury, will not penetrate the pores until sufficient pressure is applied to force its entrance, (Nagy 2005). The porosimeter measures the mercury volume, which penetrates into the samples as the applied pressure increases. The applied pressure P_s is directly related to the pore radius r into which the mercury is intruded. The relationship between the pressure P_s [Pa] and the pore radius r [m] is given by the Washburn equation, (Washburn, 1921):

$$P_s = \frac{2\gamma}{r}\cos\theta$$

where γ [N/m] is the surface tension of the liquid and θ is the angle of contact.

Figure 3 shows the Mercury Porosimeter Micromeritics Autopore IV that was used for this study.

Figure 3 – Mercury Porosimeter Micromeritics Autopore IV, Laval University, Quebec City

Figure 4 shows an example of mercury cumulative volume during the intrusion cycle and the differential intrusion d*V*/dlog(*r*) for hardened cement pastes tested for this study. Results are presented in milliliter per gram of dried samples. Results clearly show that porous volume and capillary pore size are more important when the water-to-cement ratio increases.

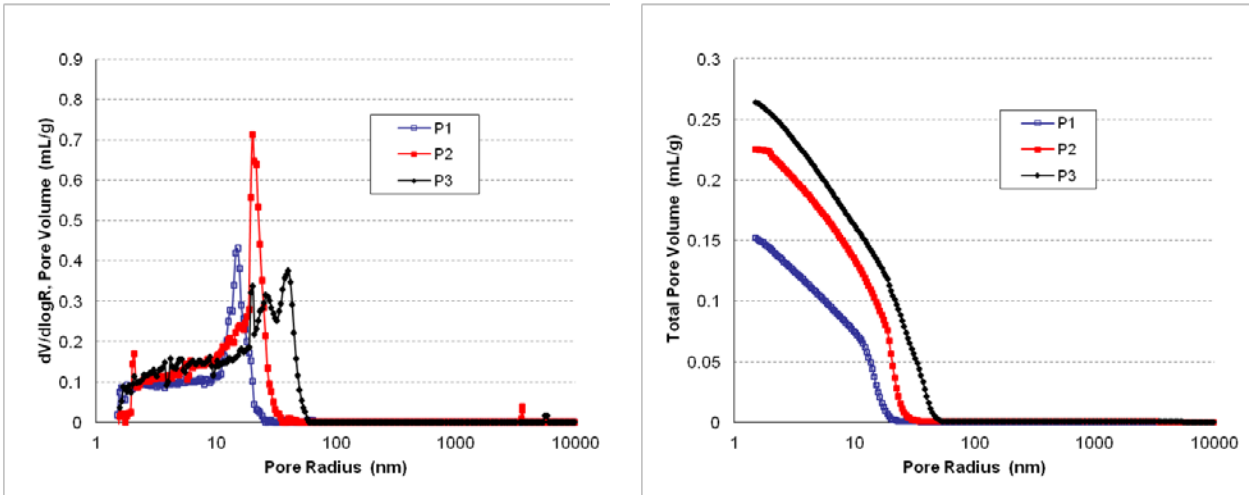

a) Differential pore volume b) Cumulative pore volume

Figure 4 – MIP measurements for hardened cement pastes P1, P2, P3

It should be mentioned that MIP is known to underestimate the total porous volume available (Abell, 1999); the finer gel (C-S-H) pores are outside the range of the pore radius measurement ($r < 5$nm).

5.0 IMMERSION TESTS

The immersion tests consisted in placing hardened cement pastes specimens in contact with a sulfate solution and evaluating the penetration of species and pore structure alteration after a certain exposure time. In the present study, all samples were exposed during three months before being removed for analysis.

5.1. Immersion in sulfate solutions

The hardened cement paste samples were immersed for three months in two contact solutions, presented in Table 5. Sodium hydroxide (NaOH) was used in one series to replicate the high-pH conditions found in the wasteform pore solution. The latter was calculated at 13.6 by SIMCO based on pore solution extraction measurements (Samson 2010). In the present study, the Na_2SO_4/NaOH solution had a pH of 13.5.

Table 5 – Exposure solution compositions

Salts	Concentrations (mmol/L)	
	Solution 1	Solution 2
Na_2SO_4	150	150
NaOH	0	500
pH	7.0	13.5

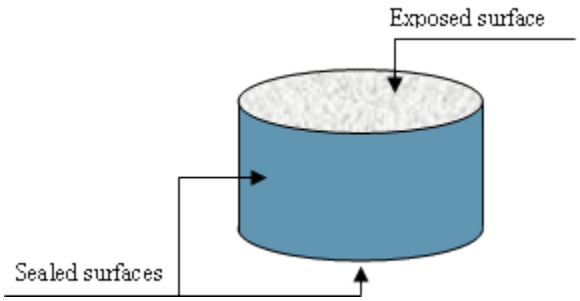

Figure 5 – Representation of a test specimen

As presented on Figure 5, 50-mm disks were cut from cylinders and sealed over all faces with wax except one flat surface. The samples were then immersed in the contact solutions. During the exposure period, the solution was renewed on a bi-weekly basis in order to maintain uniform conditions. Materials were removed from solutions after three months for analysis.

5.2. Visual observations

Hardened cement paste samples removed from solution 1 are presented on Figure 6. Some samples showed obvious visual degradation. There was a clear relationship with material quality; more damage could be observed with increasing w/c ratios.

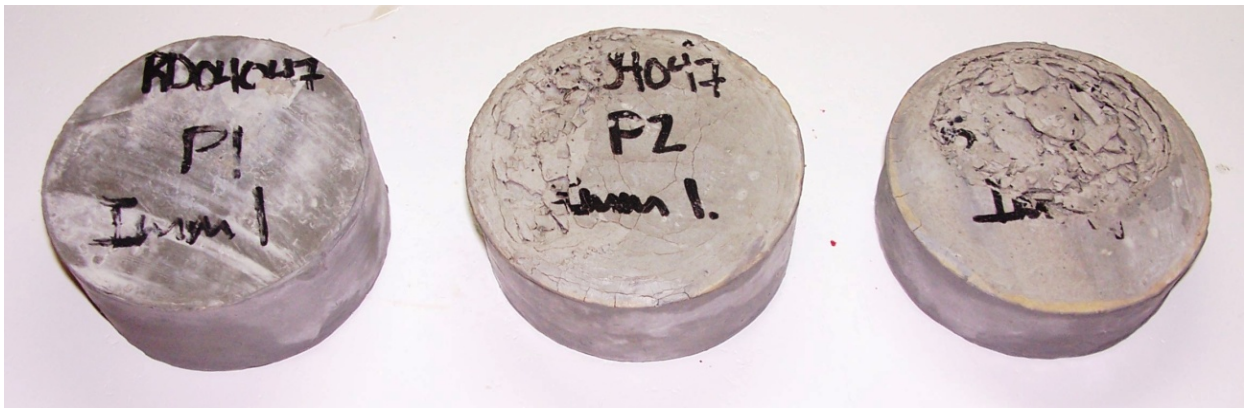

Figure 6 – Hardened cement pastes P1, P2 and P3 removed from solution 1: 150mmol/L Na2SO4 at three months

Paste P1 (w/c=0.50) did not present major visual damage. However, it was observed that the exposed surface was slightly curved as a thin layer began to be dissociated from the sample.

P2 and P3 samples showed signs of spalling after three months in the Na_2SO_4-only solution. The spalled material, around 2 mm in thickness, was brushed and removed before further analysis. Paste P2 (w/c=0.65) sample has a significant network of micro-cracks on its surface. A portion of the surface had seemingly swelled and expanded; a thin layer of 2.1 mm was partially detached from the sample. Paste P3 (w/c=0.75) sample presented a more significant deteriorated surface, an average thin layer of 2.3mm was partially detached from the sample.

Hardened cement paste samples removed from solution 2 are presented on Figure 7. In this case, no visual damage was observed on P1, P2, and P3 samples.

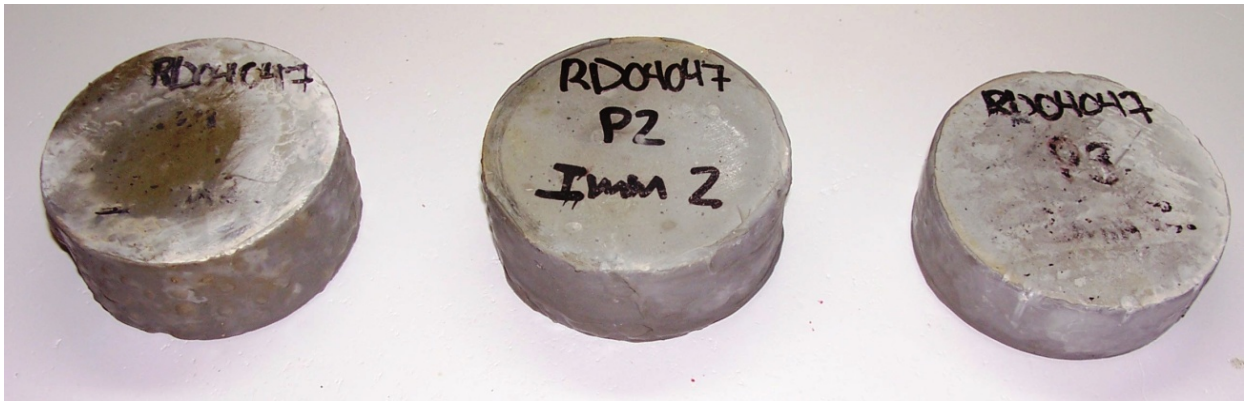

Figure 7 – Hardened cement pastes P1, P2 and P3 removed from solution 2: 150mmol/L Na_2SO_4 + 500mmol/L NaOH after three months

5.3. Sulfate content profiles

Sulfate content profiles were determined from ion chromatography and microprobe measurements. Results are presented in the next section.

Grinding/ ion chromatography analysis

Samples removed from contact solution were milled over thin layers from the exposed surface, as schematized on Figure 8. Each layer was 2-mm thick, and milling was performed over 10 layers. Powder from each layer, including the spalled surfaces, was collected and dissolved in acid on the basis of the ASTM C1152 standard procedure: Standard Test Method for Acid-Soluble Chloride in Mortar and Concrete. The resulting solution was analyzed by ion chromatography to determine the sulfate content.

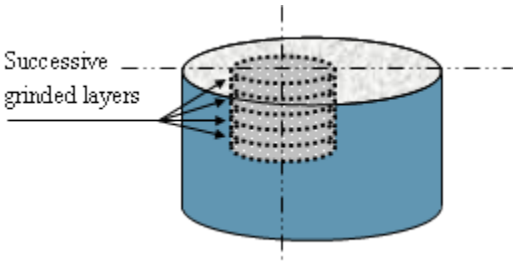

Figure 8 – Representation of successive milled layers from a test specimen

Sulfate profiles after three months in hardened cement pastes (P1, P2 and P3) exposed to solutions 1 and 2 are presented in Figure 9. Results are expressed in milligram of sulfate per gram of dried paste. On both figures, the left side of the graph (x=0) represents the paste/solution interface. Both figures show that deeper into the material, the sulfur content goes down to a constant background level, which corresponds to the amount of SO_3 present in the cement (Table 1).

These measurements clearly showed that the presence of NaOH in solution 2 limits the formation of sulfate-bearing phases in the material. Figure 9b shows that despite the high concentration of the contact solution, the sulfur level measured in all three paste samples does not extend much higher than the base level.

In the case of the low-pH contact solution 1, profiles indicate that chemical reactions near the surface resulted in the accumulation of sulfur and formation of deleterious phases. This is in line with the presence of spalling on the surface of samples in solution 1, as mentioned previously. As expected, higher w/c ratios translated into increased sulfate ingress.

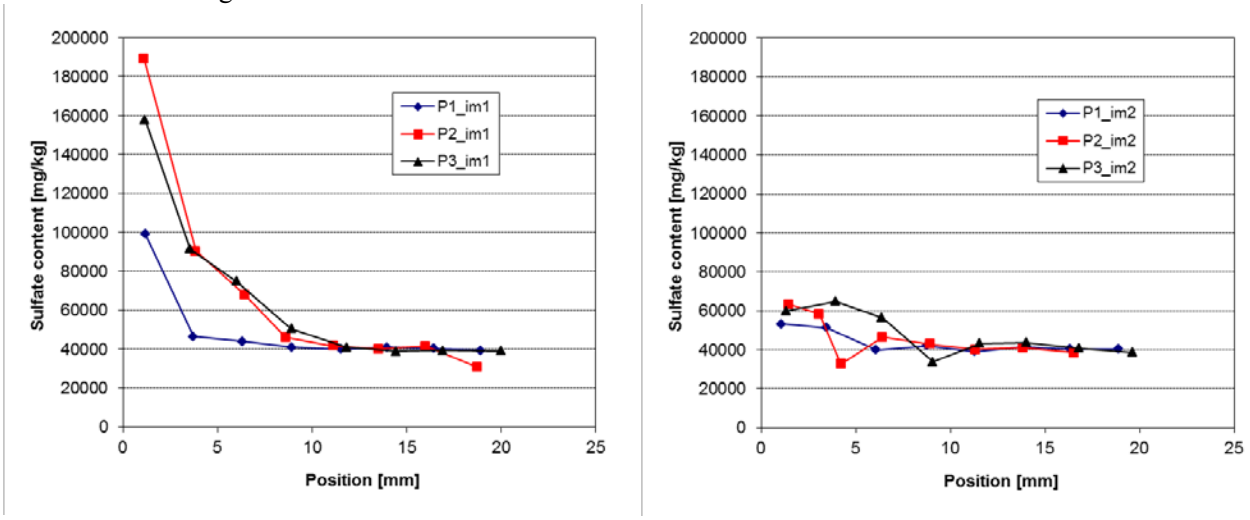

a) Na_2SO_4 exposure solution b) Na_2SO_4 + NaOH exposure solution

Figure 9 – Sulfur content in paste samples after three months

Microprobe analysis

Microprobe measurements were performed on prisms (20 x 10 x 10 mm) extracted from samples, as schematized on Figure 10. Those prisms were immersed in an isopropylic alcohol for two weeks, and dried under vacuum for two additional weeks. The samples were then impregnated with an epoxy resin, polished, and coated with carbon. They were analyzed with a microprobe, which allows determining different qualitative element contents, such as sulfur and calcium. Analysis was performed over 1,000 points along the length of the prism.

The calcium and sulfur contents were determined by electron microprobe (CAMECA SX-100) along the thickness of the sample. Sulfur profiles are presented in Figure 11. Calcium profiles are presented in Figure 18 in APPENDIX B – Microprobe Calcium Profiles.

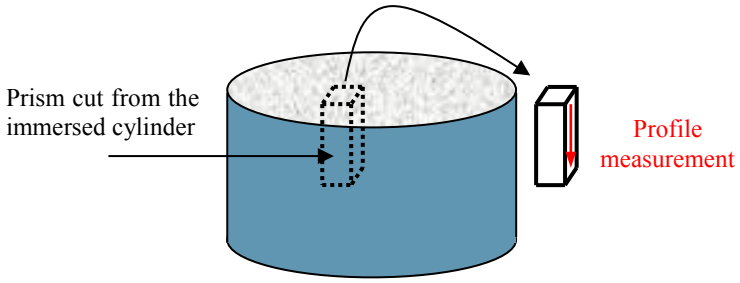

Figure 10 – Representation of a prism cut from an immersed cylinder

Sulfur profiles presented in Figure 11 also showed that the presence of NaOH in solution 2 limits the amount of sulfur in the material. Similar to the profiles showed in Figure 9b, a low amount of sulfur was measured in solution 2. The profiles also match the profiles on Figure 9 and show increasing sulfur content with increasing water-to-cement ratios.

Associated calcium profiles presented in Figure 18 in appendices provide additional information. Decalcification is observed on the first layer (from 0 to 2mm) for the Paste P1 exposed to Na_2SO_4 solution. This is a consequence of the low pH of the exposure solution, compared to the paste pore solution, which induces calcium and hydroxide leaching and causes portlandite dissolution and C-S-H decalcification. It can be safely assumed that the same observations could have been made on the other samples, had the surface layer not spalled off. Furthermore, for Paste P3, calcium seems to increase from 2 to 5mm depth. Similar observations were made on microprobe profiles presented in Samson (2007). The increase in calcium can be associated to ions dissolving near the surface and participating in the formation of gypsum and ettringite.

The presence of NaOH in solution 2 maintains a high pH in the materials, preventing the Ca-bearing phases to be dissolved. Observations on samples exposed to Na_2SO_4 + NaOH solution in Figure 18 tend to confirm that Ca profiles are relatively stables for this exposition.

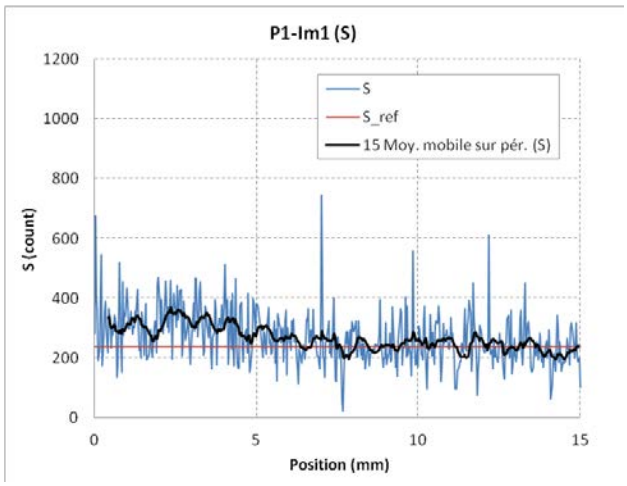

a) Paste 1, Na_2SO_4 exposure solution

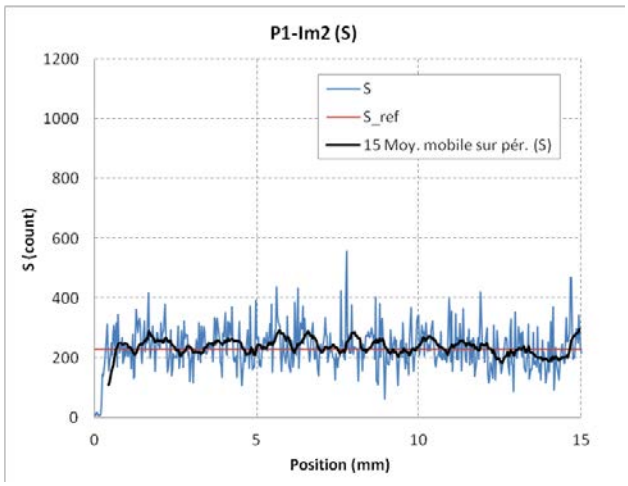

b) Paste 1, Na_2SO_4 + NaOH exposure solution

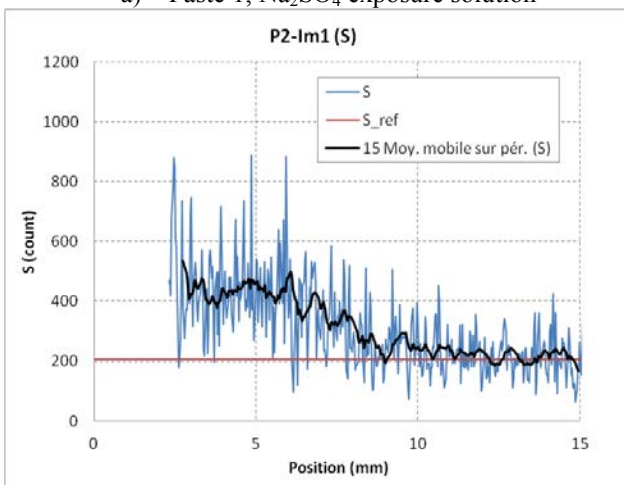

c) Paste 2, Na_2SO_4 exposure solution

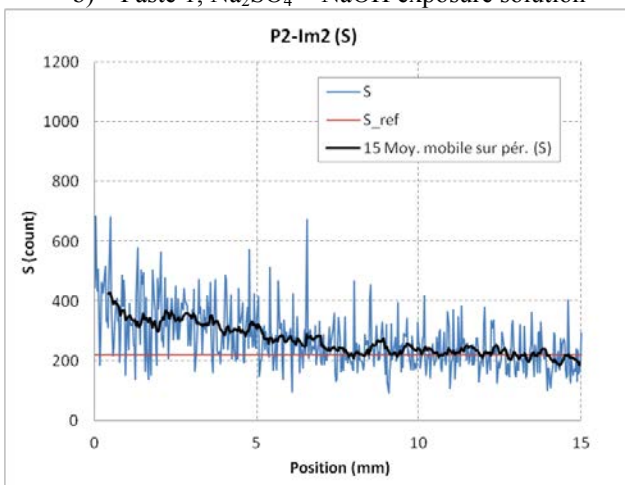

d) Paste 2, Na_2SO_4 + NaOH exposure solution

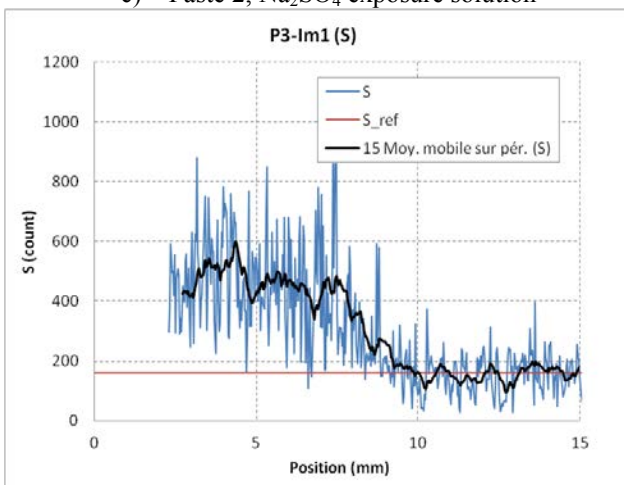

e) Paste 3, Na_2SO_4 exposure solution

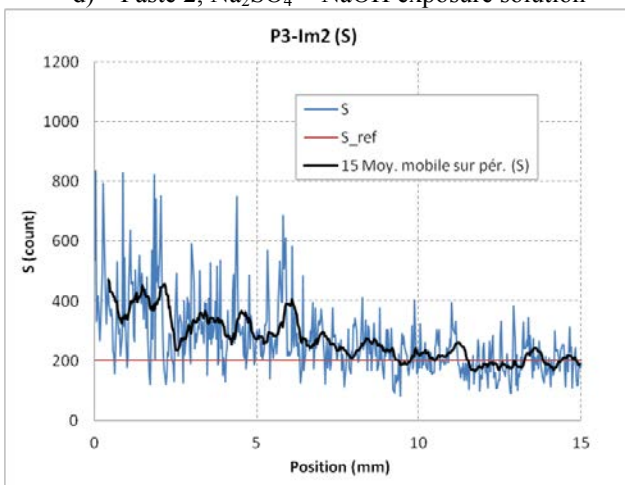

f) Paste 3, Na_2SO_4 + NaOH exposure solution

Figure 11 – Microprobe S measurements pastes immersed three months in solutions 1 and 2

5.4. Microstructure alterations

Mercury intrusion porosimetry (MIP) measurements have also been performed to quantity the pore structure evolution in the sample at different thicknesses. Samples used were extracted from cylinders presented on Figure 5, which have been immersed in solutions presented in Table 5. As presented on Figure 12, three thin pieces of approximately two millimeters were extracted from a prism previously cut from the cylinder sample to analyze the evolution of the pore structure in the material. The first layer corresponds to the top of the immersed cylinders, which have been exposed to the solution. As mentioned previously, the surface of P2 and P3 samples immersed in solution 1 was much degraded after three months of exposure. The pieces that detached from the surface were not tested for MIP analysis. In this case, the first layer corresponds to the material underneath this spalled surface.

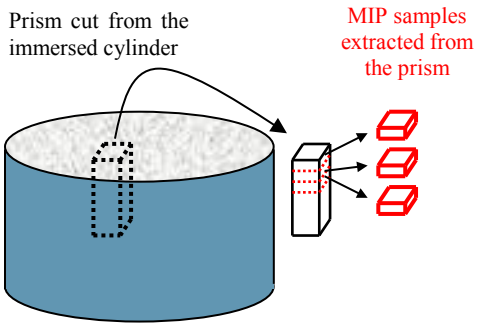

Figure 12 – Representation of MIP samples cut from an immersed cylinder

Figure 13 and Figure 14 present Mercury Intrusion Porosity results for successive layers of hardened cement pastes (P1, P2, and P3) exposed to solution 1 (Im-1, Figure 13) and solution 2 (Im-2, Figure 14). The depth and thickness of each layer is mentioned in the legend on the associated figure.

The differential intrusion dV/dlog(r) are presented in the left-side, the associated cumulative pore volume are presented in the right-side.

Figure 13 shows that the first layer of the paste samples exposed to solution 1 (Na_2SO_4 only) had a different pore size distribution. The results indicate that larger pores were created in those layers closer to the surface. This pore volume can be associated to damage (e.g.: formation of microcracks). It is particularly the case for paste P1 [0.0mm-3.0mm], paste P2 [2.2mm-4.4mm] and paste P3 [2.3mm-4.3mm] layers. It can be noted that the deeper layers identified as paste P2 [4.7mm-7.4mm], paste P3 [4.4mm-6.1mm] and paste P3 [6.4mm-8.6mm start being slightly altered for larger pore range [20nm–2µm]], compared to samples exposed to solution 2 (Na_2SO_4 + NaOH).

In addition, although a newly created pore volume appeared in larger pore range, the MIP total pore volume measured from a layer to another remains almost unchanged. The differential pore volume associated to the 10nm-100nm pore range values decreases in intensity for the top layers of materials exposed to Na_2SO_4 solution. It is particularly the case for paste P1 [0.0mm-3.0mm]; paste P2 [2.2mm-4.4mm] and paste P2 [4.7mm-7.4mm]. It is also the case for all three layers of paste P3. These observations seem to confirm that formation of phase(s) is taking place (such as gypsum/ettringite) that fills smaller pores but lead to the creation of larger pores. This suggests a damage mechanism where upon filling pore space, formation of minerals generates sufficient internal pressure to induce microcracking and open up larger pore size.

For the second contact solution (Na_2SO_4 + NaOH), no significant alteration to the pore structure could be observed, indicating that the material did not sustain significant damage, even though it was exposed to high sulfate concentrations. These observations are in line with the previous results, which show that despite a high sodium sulfate concentration, the high pH of the contact solution impedes damage formation.

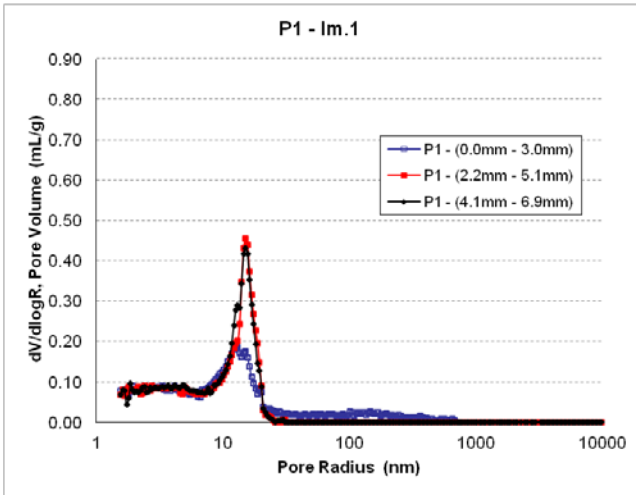

a) Paste 1, Differential pore volume

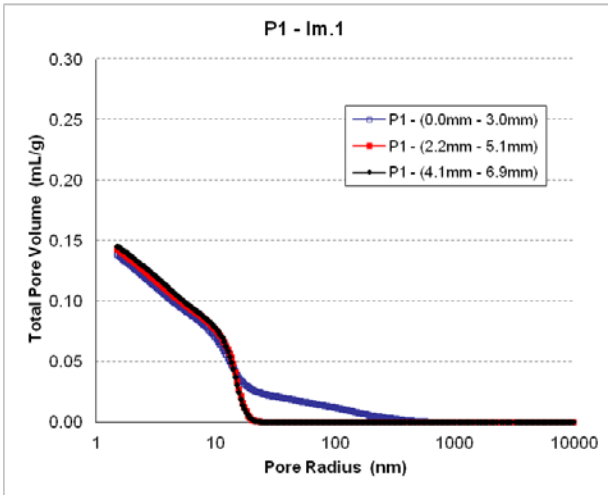

b) Paste 1, Cumulative pore volume

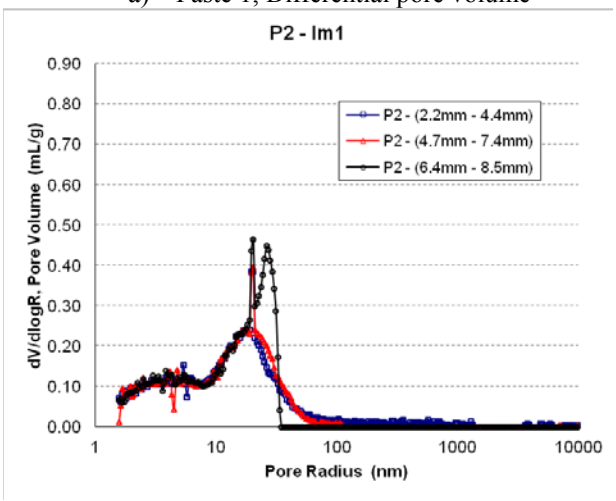

c) Paste 2, Differential pore volume

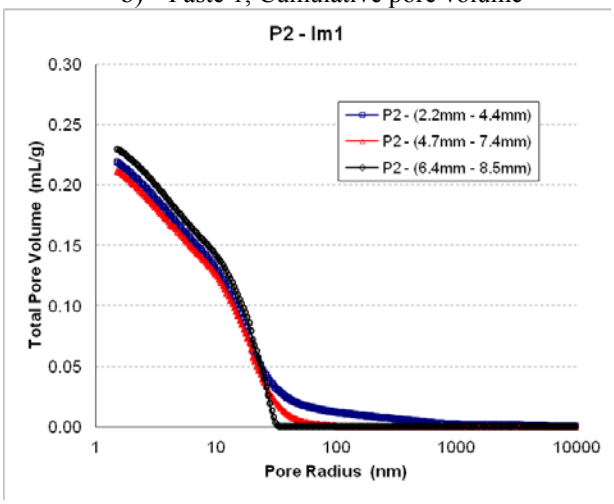

d) Paste 2, Cumulative pore volume

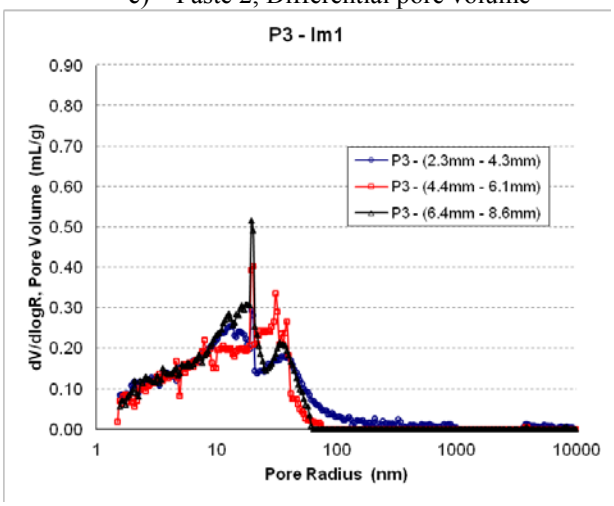

e) Paste 3, Differential pore volume

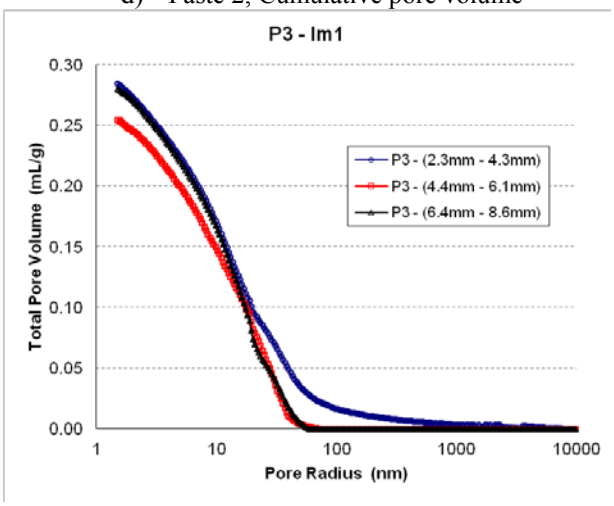

f) Paste 3, Cumulative pore volume

Figure 13 – MIP measurements for pastes immersed 3 months in solution 1, for 3 successive layers

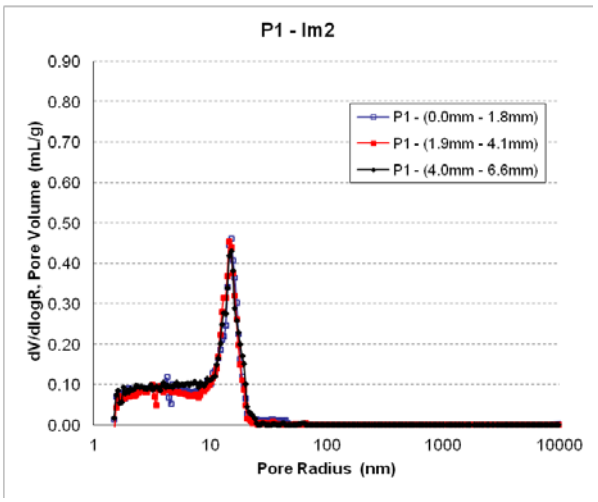

a) Paste 1, Differential pore volume

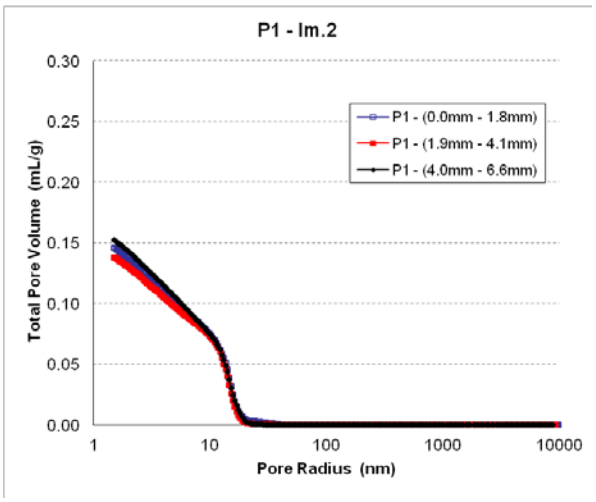

b) Paste 1, Cumulative pore volume

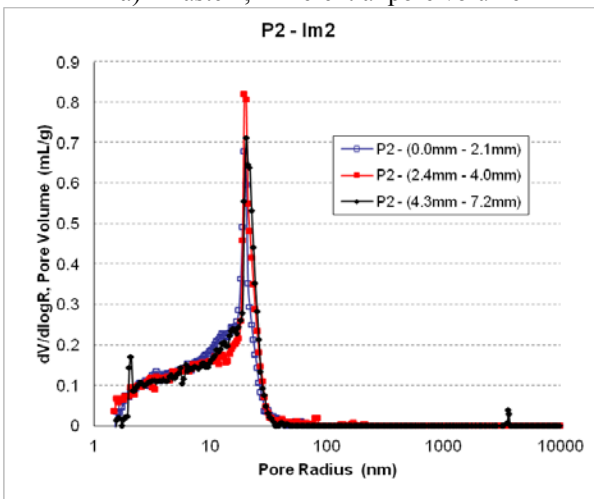

c) Paste 2, Differential pore volume

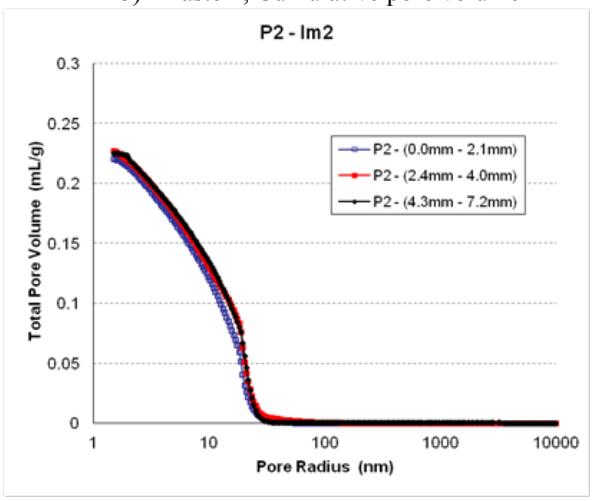

d) Paste 2, Cumulative pore volume

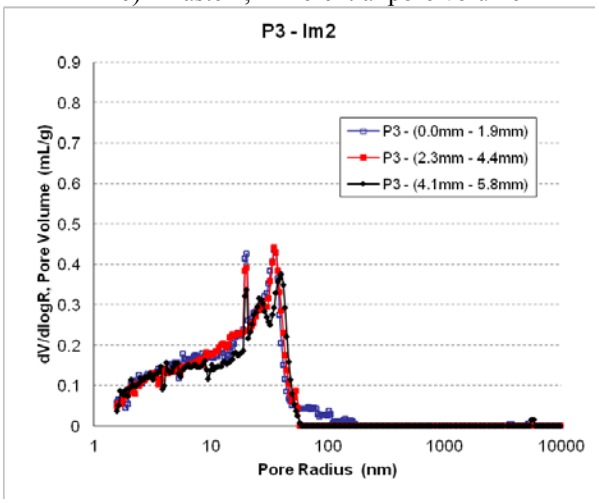

e) Paste 3, Differential pore volume

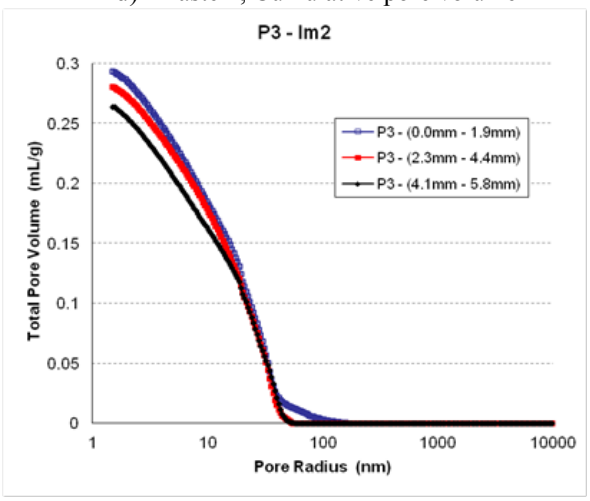

f) Paste 3, Cumulative pore volume

Figure 14 – MIP measurements for pastes immersed 3 months in solution 2, for 3 successive layers

5.5. X-ray diffraction (XRD)

Finally, XRD measurements were performed. Figure 15 shows an example of result obtained on spalled pieces from paste P2 exposed to contact solution 1, confirming that phases such as ettringite and gypsum were formed.

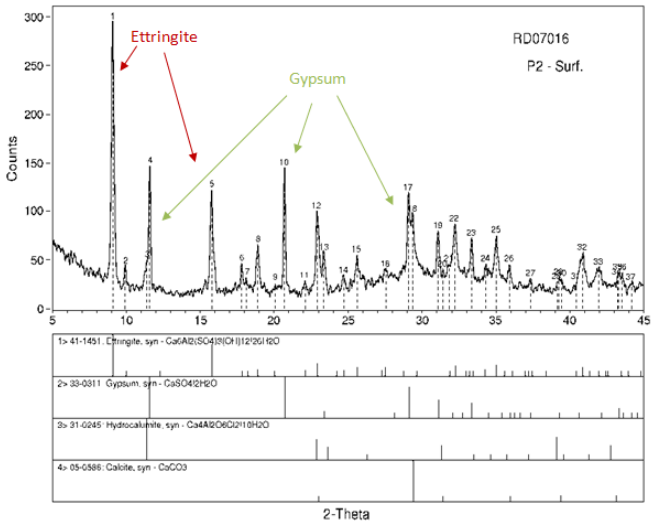

Figure 15 – XRD measurements on deteriorated surfaces for hardened cement pastes P2, immersed three months in solution 1

Schmidt (2009) also identified by scanning electron microscope (SEM), gypsum and ettringite phases on mortars exposed to Na_2SO_4. In his thesis, Kunther (2012) justified mortars expansion from sulfate attack by the formation of gypsum (or syngenite) and ettringite. Those phases were identified by SEM and energy dispersive X-ray spectroscopy (EDS) analyzes. These observations were also confirmed by phase assemblage thermodynamic modeling.

X-ray microtomography (microCT) and spatially resolved energy dispersive X-ray diffraction (EDXRD) were used in combination by Naik et al. (2006) to non-destructively monitor the physical and chemical manifestations of damage in Portland cement paste samples subjected to severe sodium sulfate attack. She also identified gypsum and ettringite as the main phases responsible for damaging cementitious materials.

6.0 DISCUSSION

The data collected so far indicate that in Na_2SO_4 solution, damage occurred to the paste. Sulfate profiles, either from layer-by-layer acid dissolution analysis or by microprobe, confirm the penetration of sulfate in the material. Limited XRD data show that in the damaged portion next to the surface, ettringite and gypsum was formed. Alterations to the microstructure were confirmed by MIP measurements. Close to the surface, where the paste is most damaged, some of the finer pored were filled, as indicated by a reduction of the pore volume in the 10nm-100nm pore range. However, for pores in the 20nm–2µm pore range, pore volume increased. This newly created volume can be associated with microcracks, likely created by the formation of ettringite and gypsum. These observations are valid for all three paste mixtures. The rate of sulfate ingress and degradation was directly related to the mix characteristics: higher water-to-cement ratio showed higher rates of degradation.

In the case of the high pH sulfate solution (Na_2SO_4 + NaOH, pH=13.5), no sign of damage was observed on any of the paste mixtures. Contrary to the previous case, the deleterious mineral phases associated with sulfate exposure did not form in the high pH environment. A possible explanation for this is the absence of gypsum formation at high pH. As shown on Figure 16, the solubility of gypsum increases with increasing NaOH concentration, thus making it more difficult for gypsum to precipitate inside paste mixes. Also, the formation of gypsum requires calcium, which comes in part from portlandite dissolution at pH 7. In the case of the Na_2SO_4 + NaOH solution, the high pH prevents portlandite dissolution, thus removing calcium for possible gypsum formation.

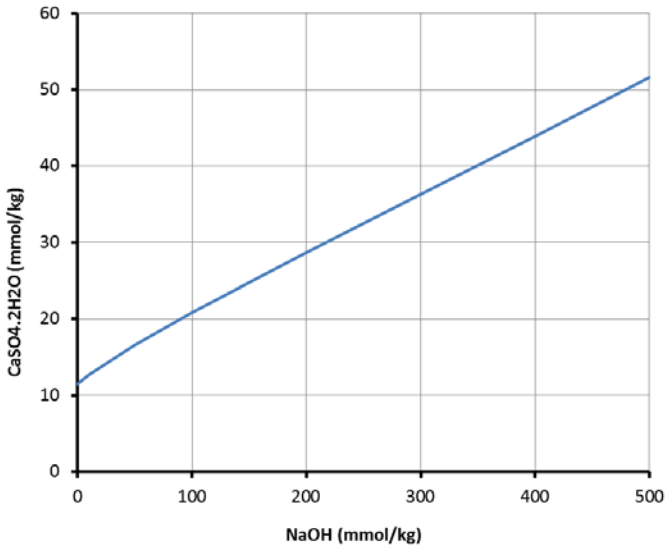

Figure 16 - Solubility of gypsum in NaOH at 25°C

Calculations made with STADIUM® to simulate contact between Saltstone and concrete as part of Task 7 of the CBP project (Samson 2010) gave similar results. As shown on Figure 17, the model predicted the formation of ettringite in the concrete barrier due to sulfate ions provided by the Saltstone. However, gypsum formation was not predicted by the model.

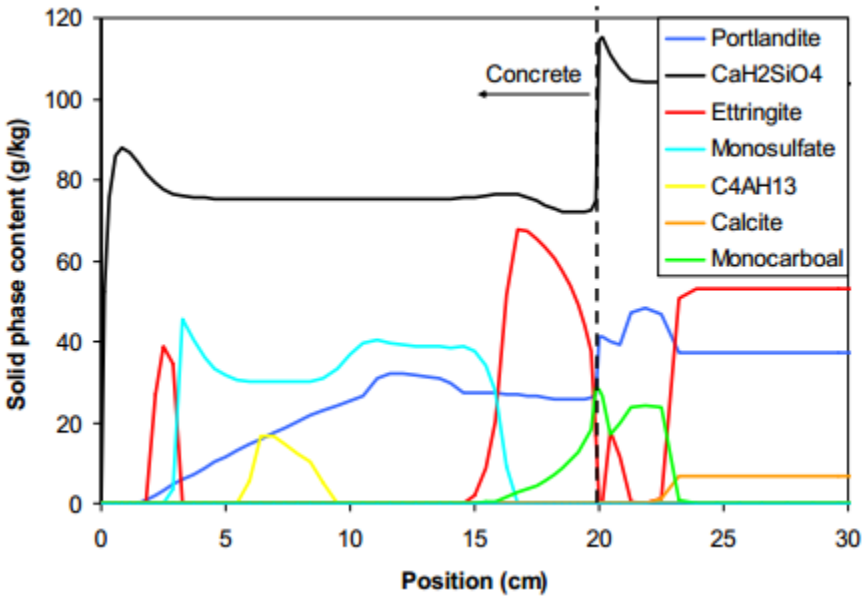

Figure 17 - Mineral distribution in concrete/Saltstone system, as obtained with STADIUM® (from Samson 2010)

There is obviously too little information to conclude that concrete will not be damaged when placed in contact with Saltstone. But it strongly suggests that the damaging mechanism will not include the formation of gypsum.

7.0 CONCLUSION

This report presented the results of an experimental study aimed at supporting the assessment of long-term durability of concrete barriers containing sulfate-bearing wasteform. The high sulfate content of the wasteform pore solution is the main cause of concern for the durability of concrete barriers.

An experimental program was designed to gather data on the effect of pH of sodium sulfate contact solutions. Hydrated paste samples prepared at different high w/c ratios were immersed in highly concentrated sodium sulfate solutions. To mimic wasteform pore solution, a sodium sulfate solution was prepared with 0.5M NaOH, resulting in a high-pH contact solution. After three months of exposure, different techniques were used to quantify the degradation sustained by the mixtures

Signs of matrix degradation were clearly seen on samples exposed to sodium sulfate. However, in the case of sodium sulfate solutions prepared with sodium hydroxide, damage was not observed. One possible explanation for this behavior is the absence of gypsum formation in high-pH environments.

Although these results need further confirmation, they indicate that the high sulfate content found in the wasteform pore solution will not necessarily lead to severe damage to concrete. Good quality mixtures could thus prove durable over the long term and act as an effective barrier to prevent radionuclides from reaching the environment. Additional experiments with contact solutions that mimic more closely wasteform pore solution are needed to confirm this.

8.0 REFERENCES

ASTM Standard C305 (2013) "Mechanical Mixing of Hydraulic Cement Pastes and Mortars of Plastic Consistency", ASTM International, West Conshohocken, PA, USA.

ASTM Standard C642 (2013) "Standard Test Method for Density, Absorption, and Voids in Hardened Concrete, ASTM International, West Conshohocken, PA, USA.

ASTM Standard C1152 (2012) "Standard Test Method for Acid-Soluble Chloride in Mortar and Concrete", ASTM International, West Conshohocken, PA, USA.

Abell A.B., Willis K.L. and Lange D.A. (1999) "Mercury Intrusion Porosimetry and Image Analysis of Cement-Based Materials", Journal of Colloid and Interface Science, 211, pp. 39-44.

Kunther W. (2012) "Investigation of Sulfate Attack by Experimental and Thermodynamic Means", PhD Thesis, École Polytechnique Fédérale de Lausanne.

Nagy V. and Vas L.M. (2005) "Pore characteristic determination with mercury porosimetry in polyester staple yarns", Fibres - Textiles in Eastern Europe, vol. 13, No 3(51) pp.21-26

Naik N.N., Jupe A.C., Stock S.R., Wilkinson A.P., Lee P.L., Kurtis K.E. (2006), "Sulfate attack monitored by microCT and EDXRD: Influence of cement type, water-to-cement ratio, and aggregate", Cement and Concrete Research, vol. 36, pp. 144-159.

Samson E., Marchand J. (2007) "Modeling the transport of ions in unsaturated cement-based materials", Computers & Structures, 85, pp. 1740-1756.

Samson E. (2010) "Cementitious Barriers Partnership Task 7 – Demonstration of STADIUM® for the performance assessment of concrete low activity waste storage structures", CBP-TR-2010-007-C3, Rev. 0.

Schmidt T., Lothenbach B., Romer M., Neuenschwander J., Scrivener K. (2009) "Physical and microstructural aspects of sulfate attack on ordinary and limestone blended Portland cements", Cement and Concrete Research, vol. 39(12), pp. 1111-1121

Washburn E.W. (1921) "The dynamics of capillary flow", The Physical Review, 17(3) pp. 273-283

APPENDIX A – Desorption Isotherm Procedure

1. Scope

This test method covers the measurement of the equilibrium water content of cementitious materials exposed to a specific relative humidity environment. This test method provides desorption isotherms.

2. Summary of Test Method

This test method consists of monitoring the mass of pre-saturated cementitious materials in a constant relative humidity environment at a constant temperature until materials reach moisture equilibrium. The different relative humidities are maintained in relatively small containers (boxes) using different supersaturated salt solutions.

3. Significance and Use

Isotherms give the equilibrium relationship between relative humidity and water content of the tested material at constant temperature.

The shape of the isotherms depends on many factors including: (a) concrete mixture proportions, (b) presence of chemical admixtures and supplementary cementitious materials, (c) composition and physical characteristics of the cementitious component and aggregates, (d) entrained air content, (e) type and duration of curing, (f) degree of hydration or age, (g) presence of microcracks, (h) presence of surface treatments such as sealers or form oil and (i) placement method including consolidation and finishing. Equilibrium water content is also a function of temperature.

4. Apparatus

4.1 Humidity boxes – One or more relatively small containers (boxes) should be prepared where saturated salt solutions are placed on the bottom of the container. The dimension of the boxes and preparation of salt solution should respect the requirements stated in ASTM E104 “Standard Practice for Maintaining Constant Relative Humidity by Means of Aqueous Solutions”. A support should be installed in each box that can properly hold the test specimens. The number of box depends on the number of relative humidities to be tested and the total amount of test specimens, which is on the user’s choice.

4.2 Balance – The balance to be used to determine the mass of the specimens during the test should have a sufficient capacity and a precision of 0.01g. The balance should be installed in a place near the humidity boxes.

4.3 Hygrometers – Small size hygrometers are needed and should be properly installed in each humidity box in order to monitor the relative humidity and temperature inside the boxes during the test period.

4.4 Device for weighing specimens in water – A device should be prepared that allow to weigh the specimens in water (Figure 1).

4.5 Towel – absorbable tissues should be prepared to remove the surface water of pre-saturated specimens.

4.6 Container and limewater – a container with certain amount of lime water inside (saturated $Ca(OH)_2$ solution) are needed to saturate the specimens before test (To make saturated $Ca(OH)_2$ solution, dissolve 3g Ca(OH) into 1 litre water.)

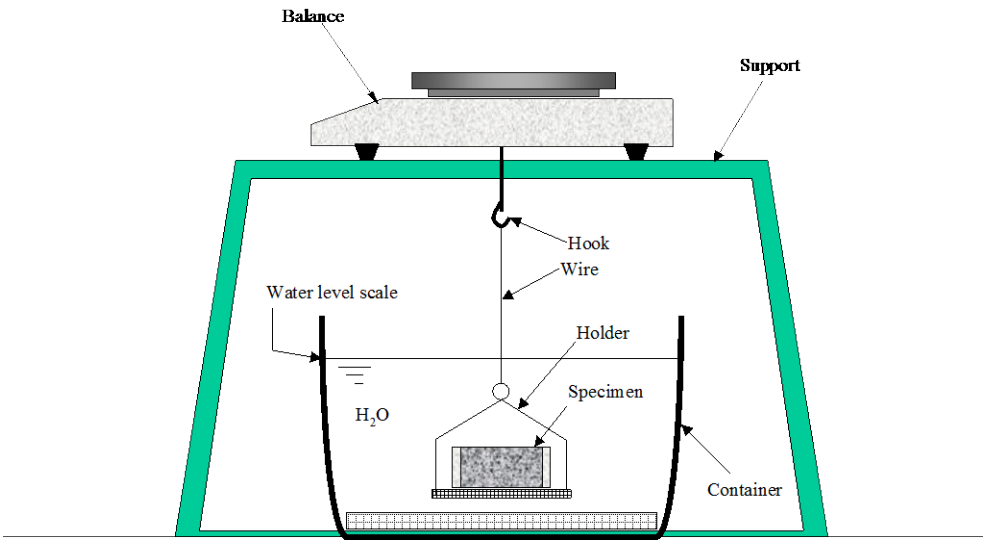

Figure 1 – Device for weighing specimen in water

5. Reagents and Materials

The salt needed depends on the relative humidity to be tested. Some salts that normally used to maintain constant relative humidities and recommended by ASTM E104 are as follows:

LiCl – for maintaining 11% R.H. at 23 ± 2°C.

$MgCl_2$ – for maintaining 33% R.H. at 23 ± 2°C.

$MgNO_3$ – for maintaining 53% R.H. at 23 ± 2°C.

NaCl – for maintaining 75% R.H. at 23 ± 2°C.

KCl – for maintaining 84% R.H. at 23 ± 2°C.

$BaCl_2$ – for maintaining 90% R.H. at 23 ± 2°C.

KNO_3 – for maintaining 94% R.H. at 23 ± 2°C.

K_2SO_4 – for maintaining 97% R.H. at 23 ± 2°C.

6. Test Specimens

6.1 Test specimens should be fully hydrated concrete (e.g., >3 months curing) to minimize possible microstructural changes during test.

6.2 Specimens should have sufficient exposed surface area and representative volume. This shall be obtained by sawing a number of thin slices from representative concrete specimens (e.g. cast concrete cylinders).

6.3 For normal weight concrete, a practical specimen should have a diameter of 100 ± 2 mm and a thickness of 10 ± 1 mm. Specimen of cement paste may be as thin as 3 to 5 mm with a section area ≥ 25 cm^2.

6.4 Minimum three (3) specimens are required for each relative humidity condition to be tested.

6.5 The test specimens should be kept constantly moist during specimen preparation.

6.6 The specimens should be fully saturated before being tested. To saturated the specimens, immerse the specimens in limewater (saturated $Ca(OH)_2$), monitor their weight (surface dry) change until constant weight is observed: weigh each specimen at time interval of 5-7 days until four successive mass determinations show mass variation <0.5% of its initial mass.

7. Procedure

7.1 All the humidity boxes to be used for the tests should be placed in a normal laboratory environment where constant temperature of 23±2°C is maintained.

7.1 Measure the dimension of each specimen to be tested : take three determinations of the thickness and two measurements of the diameter with precision of 0.01mm.

7.2 Weigh each specimen in pure water (W_1) using the device mentioned in section 4.4.

7.2 Carefully dry the surface of each specimen by absorbing the surface water using a moist tissue; then weigh it in air with precision of 0.01g, take down the initial mass of the surface dry-saturated specimen (W_0).

7.3 Properly place the specimens on the support inside the humidity box (vertically and slightly inclined position is recommended, see Figure 2) with space ≥2cm between the specimens, then, close the cover.

7.4 Weigh each of the specimen with precision of 0.01g at time interval of 5-7 days (normally one weighing per week) (Note 1). Determine the mass change between each two successive mass determinations.

Note 1: During each mass determination, the specimens should not be exposed to the environment outside the humidity box for more than one minute. If the balance is installed in a distance from the humidity box, seal the specimens in plastic bag during transportation.

7.5 Stop the test when four (4) successive mass determinations show mass change (absolute value) less than 0.5% of the cumulative mass loss during the test period.

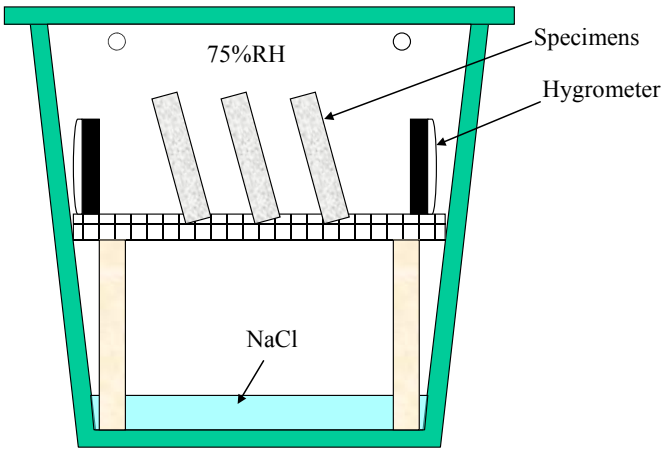

Figure 2 – Humidity box and tested specimens inside during isotherm test

8. Report

Report the following:

8.1 Information about the specimens - mixture ID and curing age of the concrete tested and porosity tested according to ASTM C642 standard procedure.

8.2 Experimental recording sheet that includes the ID of the test specimens, apparent mass in water (W_1), the initial mass of surface-dry specimens in air (W_0), date and time of each mass determination, and all the recordings of mass determination during the entire test period.

8.3 The equilibrium water content

The equilibrium water content at the relative humidity tested is calculated based on the following relationship:

$$\theta(RH)\% = \phi - 100 \times \frac{W}{V}$$

Where θ(RH) is the equilibrium water content (%) at the tested relative humidity(RH), Ø is the porosity (%) determined according ASTM C642 standard procedure , W is the cumulative mass loss (g) during the entire test period, V is the volume (cm^3) of the tested specimen ($V = W_0 – W_1$).

8.4 If more than two relative humidities have been tested, plot the equilibrium water contents obtained against the corresponding relative humidities. If more than four (4) water contents at different relative humidities have been obtained, analysis based on curve fitting may also be performed, which may provide approximation of the isotherm in larger range of relative humidity.

APPENDIX B – Microprobe Calcium Profiles

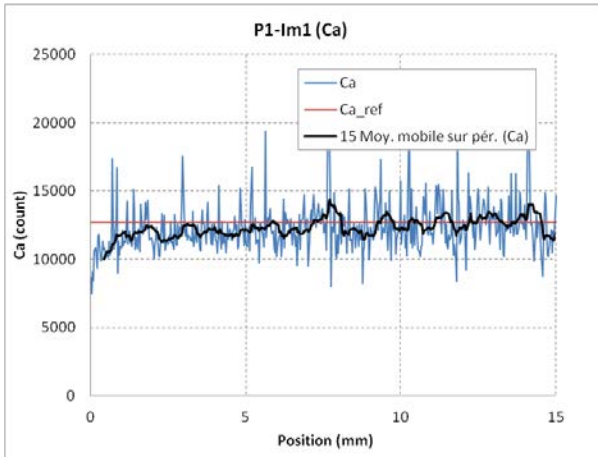

a) Paste 1, Na_2SO_4 exposure solution

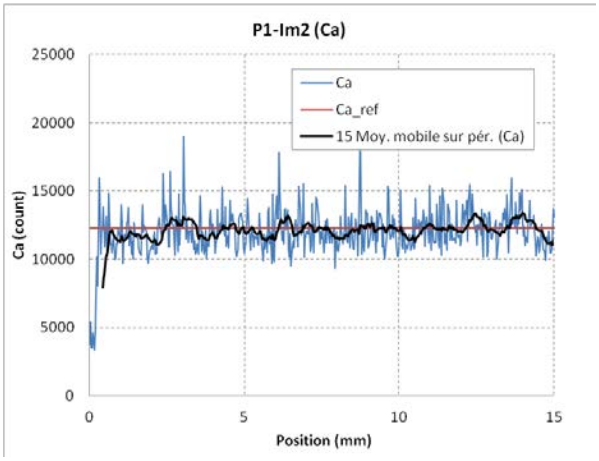

b) Paste 1, Na_2SO_4 + NaOH exposure solution

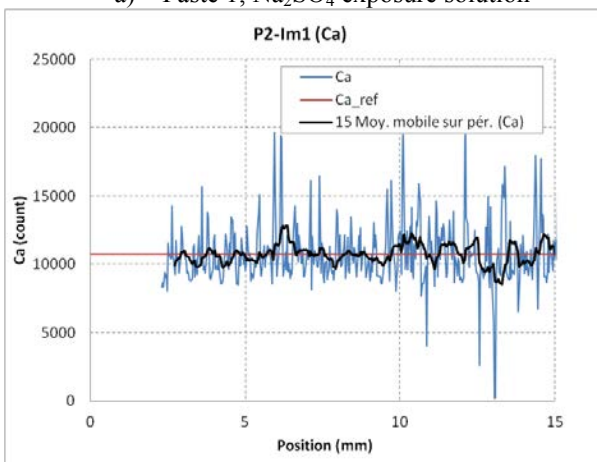

c) Paste 2, Na_2SO_4 exposure solution

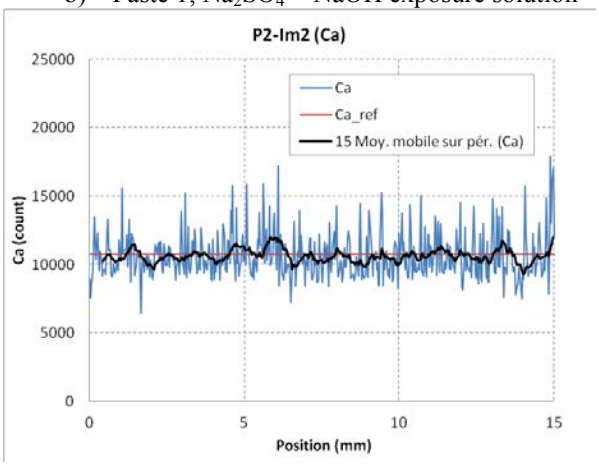

d) Paste 2, Na_2SO_4 + NaOH exposure solution

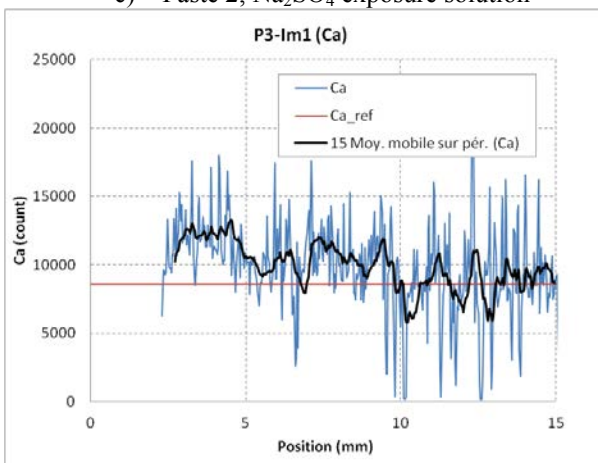

e) Paste 3, Na_2SO_4 exposure solution

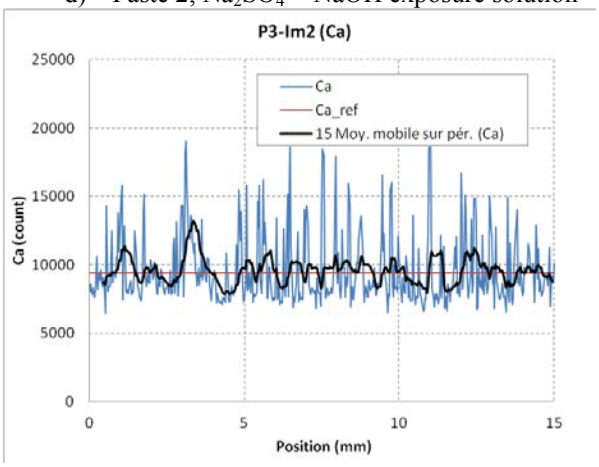

f) Paste 3, Na_2SO_4 + NaOH exposure solution

Figure 18 – Microprobe Ca measurements pastes immersed three months in solution 1 and 2.


U.S. DEPARTMENT OF
ENERGY


SRNL
SAVANNAH RIVER NATIONAL LABORATORY


CRESP


VANDERBILT
UNIVERSITY


UNITED STATES NUCLEAR REGULATORY COMMISSION


NIST
National Institute of
Standards and Technology


ECN


SIMCO
Technologies inc.